Black TiO_2 Nanotubes: Enabling Visible Light Enhancement for Enhanced Photocurrent conversion

Kang Du and Kaiying Wang[1]
[1]Department of Microsystems, University of South-Eastern Norway, Campus Vestfold, Raveien 215, 3184, Horten, Norway

Kaiying.Wang@usn.no

Titanium dioxide (TiO_2) nanotubes have emerged as a versatile platform in various fields, owing to their unique structural and functional properties. Recently, the development of black TiO_2 nanotubes (B-TNT) has garnered significant attention due to their exceptional ability to harness visible light for enhanced photoconversion processes [1]. Unlike traditional TiO_2 materials, B-TNT exhibit a distinct black coloration, attributed to the presence of oxygen vacancies and surface modifications, which enable efficient absorption of visible light [2]. This characteristic presents a paradigm shift in the field of photocatalysis and photoconversion, offering new opportunities for addressing challenges associated with conventional TiO_2-based materials, such as limited light absorption in the visible spectrum [3]. In this abstract, we aim to provide a comprehensive overview of the structural and optical properties of B-TNT, highlighting their potential applications in enhancing photoconversion efficiency and advancing sustainable energy technologies. Through a detailed exploration of B-TNT, we endeavor to elucidate their role in enabling visible light enhancement and paving the way towards next-generation photoconversion systems. TiO_2 nanotubes (TNT) electrodes were fabricated through anodization of titanium foil in a fluoride-containing electrolyte solution composed of 0.5 wt% ammonium fluoride (NH_4F), 97 vol% ethylene glycol (EG), and 3 vol% water [4]. Following anodization, the resulting material underwent annealing at 500°C for 3 hours in air to yield anatase TNT (W-TNT). Subsequently, Black TiO_2 nanotubes (B-TNT) were synthesized via electrochemical reduction in a 0.5 M Na_2SO_4 electrolyte under an applied potential of 5 V for 15 s [5]. Figure 1 illustrates the distinctive features of W-TNT and B-TNT electrodes, with the latter exhibiting a noticeable dark blue or blackish-blue coloration. The surface morphology was examined using scanning electron microscopy (SEM, Hitachi SU8230) with an accelerating voltage of 5 kV. Both W-TNT and B-TNT exhibit a porous periodic tubular structure. As depicted in Figure 2(a) and (b), there are no discernible morphological distinctions between W-TNT and B-TNT. X-ray diffraction (XRD) analysis was conducted to examine the structure and orientation of the as-prepared electrodes, as depicted in Figure 3. Both W-TNT and B-TNT exhibit diffraction peaks at 2θ values of 25.3°, 37.8°, 48.0°, 53.9°, 55.0°, 62.7°, 68.8°, 70.3°, and 75.1°, corresponding to crystal planes (101), (004), (200), (105), (211), (204), (116), (220), and (215), respectively. These peaks are characteristic of the anatase phase pattern, indicating that electrochemical reduction does not significantly alter the crystal structure or crystalline orientation. Figure 4 presents the UV–vis absorption spectra of W-TNT and B-TNT electrodes across the wavelength range of 220 nm–850 nm, measured using a UV-VIS spectrophotometer with a fine $BaSO_4$ plate as a reference. Notably, the absorption intensity of B-TNT exhibits a substantial enhancement in the visible light region, specifically from wavelengths of 400 nm–850 nm. This augmentation underscores the enhanced light absorption capability of B-TNT, particularly within the visible spectrum. The photocurrent performance of the as-prepared electrodes was assessed using an electrochemical workstation (Zahner elektrik IM6) in a two-electrode configuration. The electrodes were stacked alongside fluorine-doped tin oxide (FTO) glass. To define the illumination area, a light barrier with a radius of 1 cm (opening area: 78.5 mm^2) was placed over the FTO glass. Various light sources were utilized, including a blue laser (~10 mW/cm^2 @ 405 nm), a green laser (~10 mW/cm^2 @ 515 nm), a red laser (~10 mW/cm^2 @ 635 nm), and UV-LEDs with intensities of 14000 mW/cm^2 @ 365 nm and 15000 mW/cm^2 @ 385 nm. The photocurrent performance of the as-prepared electrodes was evaluated using an electrochemical workstation (Zahner elektrik IM6) in a two-electrode configuration, with the electrodes stacked alongside fluorine-doped tin oxide (FTO) glass. A light barrier with a radius of 1 cm (opening area: 78.5 mm^2) was placed over the FTO glass to define the illumination area. Under blue, green, red laser, and UV-LED illumination, the maximum photocurrents at the bias voltage of +4V recorded for the W-TNT electrode were 3.8 μA, 2.0 μA, 2.6 μA, and 36 μA, respectively (as depicted in Figure 5). In contrast, the B-TNT electrode exhibited maximum photocurrents of 3.5 mA, 4.2 mA, 2.2 mA, and 18 mA under the same illumination conditions (as shown in Figure 6). Notably, compared to the W-TNT electrode, the photocurrents of the B-TNT electrode were enhanced approximately 921-fold, 2100-fold, 846-fold, and 500-fold, respectively, as evidenced by the results in Figures 5 and 6. These findings underscore the significant enhancement in photocurrent exhibited by the B-TNT electrode, attributed to its pronounced light absorption in the visible regime and efficient charge separation properties.

References

[1] N. Liu, C. Schneider, D. Freitag, M. Hartmann, U. Venkatesan, J. Müller, P. Schmuki, Nano letters 14, no. 6 (2014): 3309-3313.
[2] J. Li, C.H. Liu, X. Li, Z.Q. Wang, Y.C. Shao, S.D. Wang, X.L. Sun, W.F. Pong, J.H. Guo, and T.K. Sham, Chemistry of Materials 28, no. 12 (2016): 4467-4475.
[3] L. Ji, Y. Zhang, S. Miao, M. Gong, and X. Liu, Carbon 125 (2017): 544-550.

[4] K. Du, G. Liu, X. Chen, and K. Wang, Journal of The Electrochemical Society 162, no. 10 (2015): E251.
[5] K. Du, G. Liu, X. Chen, and K. Wang, Electrochimica Acta 277 (2018): 244-254.

Figures

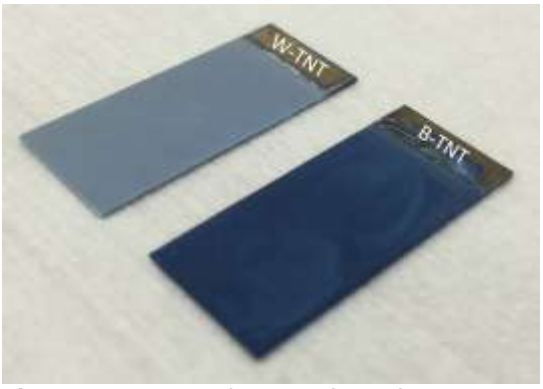

Figure 1. W-TNT and B-TNT electrodes.

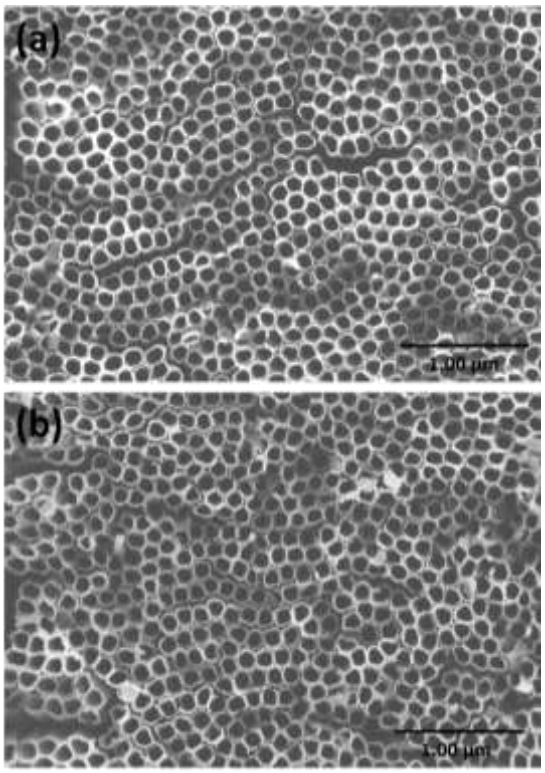

Figure 2. Surface morphologies of W-TNT and B-TNT electrodes.

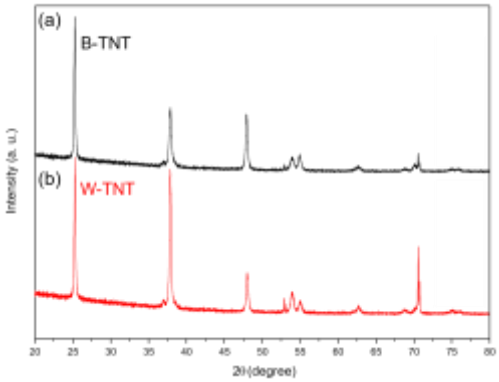

Figure 3. XRD spectra of W-TNT and B-TNT electrodes.

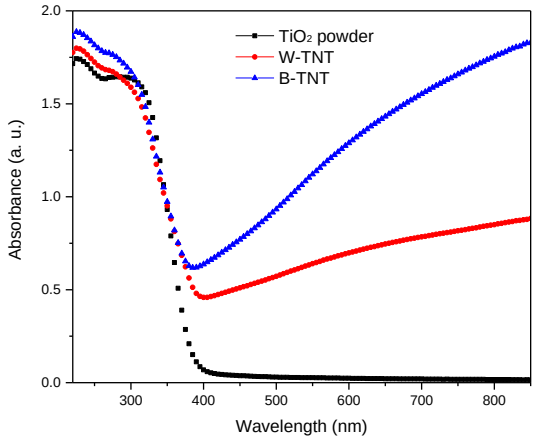

Figure 4. UV-VIS absorption spectra of W-TNT and B-TNT electrodes.

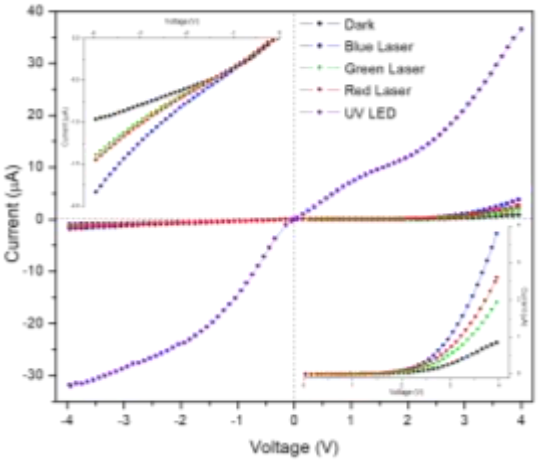

Figure 5. Photocurrent properties of W-TNT electrode under illumination of various light sources.

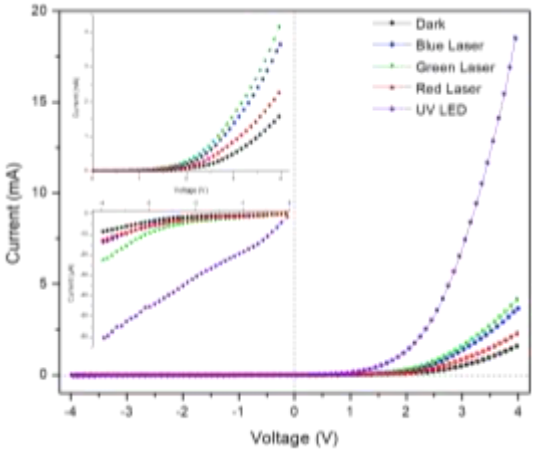

Figure 6. Photocurrent properties of B-TNT electrode under illumination of various light sources.